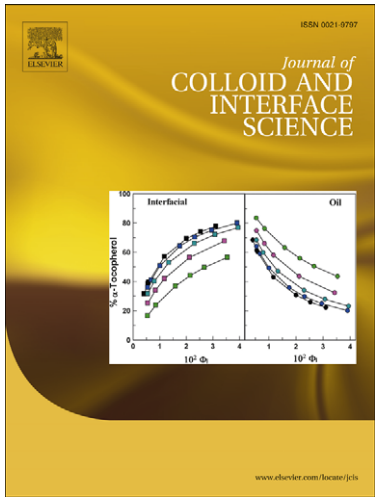

A comparative study of submicron particle sizing platforms: Accuracy, precision and resolution analysis of polydisperse particle size distributions

Will Anderson, Darby Kozak, Victoria A. Coleman, Åsa K. Jämting, Matt Trau

PII: S0021-9797(13)00175-6
DOI: http://dx.doi.org/10.1016/j.jcis.2013.02.030
Reference: YJCIS 18634

To appear in: *Journal of Colloid and Interface Science*

Received Date: 16 November 2012
Accepted Date: 11 February 2013

Please cite this article as: W. Anderson, D. Kozak, V.A. Coleman, Å. Jämting, M. Trau, A comparative study of submicron particle sizing platforms: Accuracy, precision and resolution analysis of polydisperse particle size distributions, *Journal of Colloid and Interface Science* (2013), doi: http://dx.doi.org/10.1016/j.jcis.2013.02.030

A comparative study of submicron particle sizing platforms: Accuracy, precision and resolution analysis of polydisperse particle size distributions

Will Anderson,[a] *Darby Kozak,*[a] *Victoria A. Coleman,*[b] *Åsa, K. Jämting,*[b] *and Matt Trau*[a,c]

(a) Australian Institute for Bioengineering and Nanotechnology

University of Queensland, Brisbane

Australia 4072

Fax: 61 7 3346 3973

Tel: 61 7 3346 4173

Email: Will Anderson (will.anderson@uqconnect.edu.au), Darby Kozak (darby.kozak@izon.com), Matt Trau (m.trau@uq.edu.au)

(b) National Measurement Institute Australia

Nanometrology Section

Bradfield Road

West Lindfield

Australia 2070

Fax: 61 2 8467 3752

Tel: 61 2 8467 3700

Email: Victoria Coleman (Victoria.Coleman@measurement.gov.au), Åsa Jämting (Asa.Jamting@measurement.gov.au)

(c) School of Chemistry and Molecular Biosciences

University of Queensland, Brisbane

Australia 4072

Fax: 61 7 3346 3973

Tel: 61 7 3346 4173

Corresponding Author:

Will Anderson

Australian Institute for Bioengineering and Nanotechnology

University of Queensland, Brisbane

Australia 4072

Fax: 61 7 3346 4161

Tel: 61 7 3346 4173

Email: will.anderson@uqconnect.edu.au

Abstract

The particle size distribution (PSD)[1] of polydisperse or multimodal system can often be difficult to obtain due to inherent limitations of a measurement technique. For this reason, the resolution, accuracy and precision of three new and two established, commercially available and fundamentally different particle size analysis platforms were compared by measuring individual and a mixed sample of monodisperse sub-micron (220, 330 and 410 nm - declared modal size) polystyrene particles. The platforms compared were the qNano Tunable Resistive Pulse Sensor, Nanosight Particle Tracking Analysis System (model #) the CPS Instruments UHR24000 Disc Centrifuge, and the routinely used Malvern Zetasizer Nano ZS Dynamic Light Scattering and Transmission Electron Microscope platforms . All measurements were subjected to a peak detection algorithm so that the detected particle populations could then be compared with to Transmission Electron Microscope

[1] Abbreviations used: Coefficients of Variation (CV%), Differential Centrifugal Sedimentation (DCS), Dynamic Light Scattering (DLS), Tunable Resistive Pulse Sensor (TRPS), Full Width at Half Maximum (FWHM), Particle Size Distribution(s) (PSD(s)), Particle Tracking Analysis (PTA), Percentile values 10, 50 and 90 % (P10, P50, P90), Polystyrene particles with diameters of 220 nm, 330 nm, 410 nm, (PS220, PS330, PS410), Standard Electrolyte Buffer (SEB), Standard Deviation (SD), Transmission Electron Microscopy (TEM).

measurements of the individual particle populations. Of the four techniques, only the Tunable Resistive Pulse Sensor and Disc Centrifuge provided the resolution required to detect all three particle populations present in the mixed 'multimodal' particle sample. In contrast, the light scattering based Particle Tracking Analysis and Dynamic Light Scattering techniques were only able to detect a single population of particles corresponding to either the largest (410 nm) or smallest (220 nm) particles in the sample, respectively. When the particle sets were measured separately (monomodal) each technique was then able to resolve and accurately obtain a mean particle size within 10 % of the Transmission Electron Microscope reference values. However, the broadness of the PSD measured in the monomodal samples deviated greatly, with coefficients of variation being ~2–6 fold larger than the TEM measurements across all four techniques. The large variation in the PSDs obtained from these four, fundamentally different techniques indicates that great care must still be taken in the analysis of samples known to have complex PSDs. All of the techniques were found to have high precision, i.e. they gave rise to less than 5 % variance in PSD shape descriptors over the replicate measurements.

Keywords: multimodal, nanoparticle, characterization, Malvern zeta sizer, dynamic light scattering, qNano Tunable Resistive Pulse Sensor, Nanosight particle tracking analysis, CPS disc centrifuge, transmission electron microscopy

Introduction

Many submicron particle suspensions have complex particle size distributions (PSD) [1], in that the size distribution is broad (polydisperse), or they consist of several distinct particle populations of varying size (multimodal). Currently, most particle sizing techniques are only able to accurately measure an average particle size for simple monomodal systems [2-5]. For example, Bell et al. [6] recently demonstrated that 6 submicron particle sizing techniques, being, an Tunable Resistive Pulse SensorTunable Resistive Pulse Sensor (TRPSTRPS), Particle Tracking Analysis (PTA), Differential Centrifugal Sedimentation (DCS), Dynamic Light Scattering (DLS), Transmission Electron Microscopy (TEM) and Scanning Mobility Particle Sizing (MonoPS), generated similar mean values for the PSDs of several monomodal, submicron, Stöber silica particle suspensions. In contrast, obtaining the 'true' PSD of a multimodal or polydisperse sample is often more challenging due to fundamental limitations in the detection and analysis methodologies of current sizing techniques. For example, it is well known that techniques such as light scattering, optical microscopy and electron microscopy are limited because they either measure only an averaged sample size distribution, lack the resolution to observe such small particles, or are too time consuming to be conveniently used to

measure polydisperse or multimodal samples. These factors can result in skewed or misleading representations of the true PSD of a sample.

Herein we compare the resolution of three new particle measurement platforms, TRPS, PTA and DCS, for measuring the PSD of a highly polydisperse, multimodal mixture of 220 nm (PS220), 330 nm (PS330) and 410 nm (PS410) polystyrene particles mixed in a weight ratio of 1:1:1. The size resolution of a technique is assessed by its ability to detect the three separate particle sets present in the multimodal sample, while technique accuracy is assessed from the deviation of PSD shape descriptors to those obtained from measurements of the monomodal particle sets by both TEM and each respective technique. Precision is assessed by repeatability of the measured PSD descriptors over several replicate measurements. Analysis of the theory behind each technique and the ways in which the PSD data from each technique was processed is also presented for the purpose of explaining how comparisons between the dissimilar techniques are made.

Measurement techniques

Transmission electron microscopy

TEM is an established technique that is capable of imaging samples based on the absorption of an electron beam as it passes through ultrathin (~<100 nm) samples. The transmitted beam is typically projected onto a phosphorescent screen or detector enabling micro and nanometer sized objects to be visualized. It has been a cornerstone of particle analysis for the last 50 years [7] and is widely applied for particle sizing. When applied to PSD analysis, TEM is a single particle technique that provides the added benefit of information on particle shape and composition. Particle size is measured in TEM from the diameter determined from a 2D projected area of a three dimensional particle. There are many possible diameters that can be reported, however the equivalent spherical diameter or the Feret diameter are the most common. In the case of spherical particles, all of the possible diameter measurements should be the same, however for irregularly shaped particles, the choice of equivalent diameter can produce significant variations in the results reported.

Despite the obvious benefits of being able to visually image a sample at hand, the technique is often considered to be labor intensive as many hundreds or thousands (depending on the broadness of the PSD and the desired error) [8] of particles should be measured to obtain a statistically significant PSD measurement. In order to increase the throughput of PSD measurements, automated image analysis software is often used to increase measurement throughput, however the requirement for user defined measurement parameters in these programs can often result in bias in PSD

measurements [9, 10]. A further limitation of TEM is that it requires a high vacuum environment, preventing in situ sample analysis. The high energy electron beam used in TEM can also cause damage to a sample and must be taken into consideration, particularly for biological samples (which require chemical fixing to prevent sample destruction [11]) or polymer based samples which can shrink or charge under the electron beam.

Together with the low sample throughput, poor statistics, sample preparation requirements, harsh measurement conditions and inability to measure particles in situ, the requirement for rapid, bench-top PSD determination has lead to the development of many alternative sizing techniques, which are compared in this paper.

Dynamic light scattering

DLS, or photon correlation spectroscopy (PCS), is an established and popular technique for determining PSD and has been used as a particle characterization work horse since its development in the 1960s due to its applicability to a wide spectrum of particles and dispersion media and ease of use. DLS is an ensemble measurement that determines the average hydrodynamic diameter of a particle suspension by measuring the changes in the speckle pattern produced by particles scattering light as they undergo Brownian motion. Monodisperse suspensions produce an intensity autocorrelation function, $G_2(\tau)$, that can be described by [12]

Equation 1 $$G_2(\tau) = A\left[1 + B \cdot e^{\left(-2Dq^2\tau\right)}\right]$$

where τ is the time delay between intensity measurements, A and B are the baseline and intercept of the correlation function, D is the diffusion coefficient and $q = \left(4\pi n / \lambda\right)\sin\left(\theta / 2\right)$, where n is the refractive index of the solvent, λ is the wavelength of the laser and ϑ is the scattering angle. For short time delays in τ the intensities will be highly correlated, while for long delays the correlation between intensity measurements will decay due to the movement of the particles undergoing Brownian motion. For a monodisperse system, the measured diffusion coefficient can then be related to the hydrodynamic diameter using the Stokes-Einstein equation.

Equation 2 $$d_H = \frac{kT}{3D\pi\eta}$$

where d_H is the particle's hydrodynamic diameter, k is the Boltzmann constant, T is the temperature and η is the viscosity of the medium.

For a polydisperse sample, the correlation function is described by the sum of the exponential decays of the different populations of particles present in the sample. Unfortunately, inversion of

this function to obtain the distribution of decay rates suffers from low resolution due to the ill-posed nature of the Laplace inversion [12]. To overcome this limitation a range of algorithms have been developed, such as Cumulants analysis, Non-negative least squares (NNLS) and CONTIN, that can be used to more reliably obtain information about the PSD of a polydisperse system. A more detailed analysis of DLS and the various algorithms can be found in the following articles [12, 13]. To determine the volume or number-based PSD of a sample, these algorithms additionally require *a priori* knowledge of the optical properties of both the particle and its suspending medium.

A major limitation of DLS is that it is inherently sensitive to the presence of larger particles in a sample. This is because scattered light intensity is dependent on particle size. Using the Rayleigh approximation, the intensity, *I*, of scattered light is proportional to the sixth power of the particle diameter *d*, $I \propto d^6$ [12].Thus even a few large particles in a sample will dominate the signal, resulting in an over-estimate in the mean diameter [4, 14, 15]. For this reason, DLS is not suitable for PSD analysis of highly polydisperse samples. However, the ease of use, high throughput nature, and the ability to analyze a large range of particulate sizes, materials and dispersion media has made DLS one of the most common and simplest measurement techniques for PSD determination.

Tunable Resistive Pulse Sensor

TRPSs offer a new method for PSD analysis based on a size-tunable pore that measure objects via resistive pulse sensing. Resistive pulse sensors, or Coulter counters, were first pioneered in the 1950's by W.H Coulter for high throughput, automated blood cell counting and sizing [16]. Historically, resistive pulse sensors have been limited to characterizing micro-particles, however recent advances in nanofabrication techniques and the application of biological pores, such as the α-haemolysin trans-membrane protein, have led to a resurgence in this technique as a method for *in-situ*, high throughput, single particle characterization [17-20]. In general, resistive pulse sensors measure the increased electrical resistance brought about by a particle passing through a pore filled with a conductive fluid. In the simplest case, where a spherical particle translocates across a cylindrical pore, the relative change in resistance, $\Delta R / R$ is described by [21]

Equation 3 $$\frac{\Delta R}{R} = \frac{d^3}{D^2 L}$$

Where *d* is the particle diameter, *D* is the pore diameter and *L* is the pore length. It can therefore be seen that this technique measures a number distribution of particle volumes and that it is highly sensitive to changes in particle diameter. For more complex particle and pore geometries, a range of deviation factors must be taken into account [17].

The TRPS differs from the classic Coulter counter as it utilizes a size-tunable pore that is formed by mechanically puncturing a micron sized pore into an elastic membrane [22]. Despite being a relatively new particle size analysis device, this technique is already showing promise, recently demonstrating good agreement when compared against laser diffraction, atomic force microscopy and scanning electron microscopy when measuring the PSD of superparamagnetic iron-oxide containing lipid microcapsules [23]. The pore diameter can be changed, or 'tuned', in real-time by radially stretching the membrane. Tuning the pore size has been shown to improve measurement sensitivity and resolution [24]. The ability to change pore geometry, however, makes direct measurement of particle size difficult due to the constantly changing pore size making absolute measurements difficult. Although direct measurements are possible by knowing the pore geometry at the stretch used [25], a calibration method using particles of known volume is the preferred method to obtain accurate particle size analysis [26]. The calibration method utilizes the linear relationship between the change in resistance and volume of the particle as outlined in Equation 3, and therefore a simple one-point calibration has been found to produce highly accurate and precise size analysis as long as pore dimensions are not changed [26]. A inherent disadvantage for pore based sensors is the issue of pore blockages due to particles that are either too large to fit through the pore or particles that are attracted to the pore surface, resulting in aggregate within the pore. Pore blockages limit the effective size range that can be measured by this technique and consistent blocking can result in time consuming disassembly and cleaning of the apparatus. Due to this limitation, unstable or extremely polydisperse, such as those often found in biological samples, may be difficult to analyze by TRPS. Small particles may also go undetected if they do not displace an appropriate volume of electrolyte to create a significant enough resistive pulse event. However, due to the ability to alter pore geometry in TRPS, these pores provide a greater dynamic range of analysis. Considerations must also be made to run an appropriate electrolyte that is both conductive enough to allow for resistive pulse events to occur, but also one that does not cause adverse effects to the sample, such as particle aggregation due to high salt concentrations. A recent review on TRPSs and the associated technique can be found in the book chapter by Willmott et al. [27].

Particle tracking analysis

PTA determines the hydrodynamic diameter of individual particles in a similar fashion as DLS. That is the particle diameter is calculated via the Stokes-Einstein equation (Equation 2) by directly measuring their diffusion coefficients as they undergo Brownian motion. Particles with dimensions less than the wavelength of light can be visualized under a microscope due to Mie scattering of light from an incident laser light source. The instrument software simultaneously tracks multiple particles as they enter and exit the plane of focus. Unlike DLS, the ability to track individual particles reduces

the influence of the scattered light intensity from larger particles skewing the measured PSD, making this method more capable of detecting individual particle populations in multimodal samples [28]. A potential disadvantage of PTA is that it is highly susceptible to user bias in setting up the imaging conditions [6]. Additionally, measurement times may exceed those of DLS, due to the need to make multiple measurements in order to generate sufficient statistics. An advantage of using a laser to illuminate the particles is that, for appropriate wavelengths, it is possible to study fluorescence behavior in addition to the particle size measurements and thus complement the analysis. This was recently demonstrated for fluorescent liposomes dispersed in blood [29].

Differential centrifugal sedimentation

DCS measures a PSD from the sedimentation time of particles injected into the centre of a spinning disc. Under typical operation, the disc is loaded with a sucrose solution, through which a density gradient form as the disc spins. Under these conditions, particles injected into the centre of the disc will separate according to differences in their size, density and shape, according to Stokes law [30]. In general, the equivalent spherical diameter (or "Stokes diameter"), d_S, of a particle can be calculated by;

Equation 4

$$d_{\mathrm{S}} = \left(\frac{18\eta \ln\left(\frac{R_{\mathrm{f}}}{R_0}\right)}{t\left(\rho_{\mathrm{p}} - \rho_{\mathrm{f}}\right)\omega^2} \right)^{0.5},$$

where η is the viscosity of the fluid medium, R_f is the radial position of the detector, R_0 is the radial position of the surface of the density gradient carrier fluid, t is the time taken to reach the detector located at R_f, ρ_p is the particle density, ρ_f is the fluid density and ω is the rotation speed. A particle calibration standard of known density and diameter is often used to determine the instrumental measurement constants instead of making a measurement from first principles. The extinction of light from a laser is used to monitor the amount of material moving past the fixed detector position as a function of time. In order to obtain the volume or number PSDs, the optical properties of the system must be known to convert extinction of light caused by scattering using Mie theory [31].

DCS provides the advantage of high-resolution separation (within 3%) of particle sizes over a broad size range [32]. The major limitations of this technique is that it requires reference materials for calibration, knowledge of the system parameters (including density and optical properties), making it best suited for samples of homogenous composition.

Experimental procedure and materials and method of analysis

Particles and buffers

220 nm P(S/V-COOH) 10 % w/v (PS220), 330 nm P(S/7.5 % MAA) 9.6 % w/v (PS330), and 410 nm P(S/V-COOH) 10.1 % w/v (PS410) polystyrene particles were purchased from Bangs Labs (IN, USA). Particle dispersions were prepared specifically for each technique as outlined below. All multimodal samples were prepared as a 1:1:1 weight-equivalent dispersion of the PS220, PS330 and PS410 particle sets. Samples were suspended in MilliQ water with or without 5-10 mM NaCl or a Standard Electrolyte Buffer (SEB) (0.1 M KCl, 15 mM Tris buffer, 0.01 % v/v Triton X-100, and HCl to adjust to pH 8). The samples were vortexed and sonicated > 10 min for each sample. All reagents were purchased from Sigma-Aldrich (AUS) unless otherwise stated.

Transmission Electron Microscopy

0.01 wt% of particles were suspended in EtOH and 2 µl was drop cast onto polyvinyl formal coated 200 mesh Copper TEM grids (ProSciTEch, Qld, Australia) and allowed to evaporate at room temperature. Particles were imaged at a magnification of 40 000 times using a JEOL 1010 TEM (accelerating voltage, 100 kV). Equivalent spherical particle diameters were calculated from the particle area using the automated particle detection feature of the ImageJ image analysis software (Version 1.44P). Exactly 500 individual (i.e., non-touching) particles were measured for each particle set to ensure that any influence from overlapping particles did not affect the results. Calculations of the mean, mode, CV% and percentile values of the number-based PSDs were made from the individual particles measurements.

Dynamic Light Scattering

DLS measurements were performed on the monomodal and multimodal samples using a Malvern Zetasizer Nano ZS. The stock suspensions were diluted to 0.001 wt% in 10 mM NaCl. Particle samples were allowed to equilibrate at 25 °C for 5 minutes to ensure temperature homogeneity prior to making 5 measurements, each consisting of 10 individual runs. The viscosity and refractive index values used were; 0.8872 cP and 1.330, respectively, as provided in the Zetasizer software (V. 6.20). The refractive index and absorption values for the polystyrene particles used to calculate volume and number size distributions were 1.590 and 0.001, respectively, as provided in the Zetasizer software. The data was analyzed using the General Purpose Model (GPM) algorithm, with a size range analysis of 0.1 – 10000 nm. Reasoning for using this algorithm is provided in the results and discussion section. The mean, mode, CV% and percentile values of the number-based PSDs were calculated, with the frequency % values of log bins being used as weights, with a weighted degree of

freedom, for the mean and CV% calculations. Please see the supplementary information for the statistical analyses used in this study.

Tunable Resistive Pulse Sensor

TRPS measurements were performed on an Izon qNano. Samples were prepared by diluting the stock single and multimodal particle suspensions in SEB to 0.01 wt%. The measurements were made with at least 1000 particles being detected for the monomodal runs and 2000 particles being measured for the multimodal runs. Each sample was run in triplicate. The pulse signal was calibrated with a 355 nm polystyrene particle standard supplied by Izon Science. The membrane pore size used for these experiments was rated for 100-1000 nm particles. Measurements were made with 5 mm of stretch being applied to the elastic membrane and a potential 0.9 V being applied across the pore. 40 µl of the particle/SEB mixture was loaded into the top fluid cell and 80 µl of only SEB into the bottom fluid cell. 500 Pa of pressure was applied to the top fluid cell using Izon's variable pressure unit to help facilitate the translocation of particles through the elastic pore. Calculations of the mean, mode, CV% and percentile values of the number-based PSD were made from the individual particle measurements.

Particle Tracking Analysis

Data was collected using a Nanosight LM 10 cell (red laser, 633 nm) and a Marlin CCD camera using Nanosight software (V. 2.2). Particle samples were prepared by diluting the stock suspensions to 0.01 wt% in SEB. Triplicate measurements were made for each sample. To ensure that different particles were analyzed for each replicate, a few µl of sample suspension was injected into the LM10 cell between replicates to displace the previously measured sample. Each replicate consisted of 5 repeat measurements of ~2000 particles. Data was output as the concentration distribution of particles of different diameters with bin widths of 1 nm. The concentration values were then normalized to a number-based frequency PSD at 5 nm bins. Calculations of the mean, mode, CV% and percentile values were made from the concentration distribution with 1 nm bins, the concentration distribution values were used as weights, with a weighted degree of freedom, for the mean and CV% calculations as described in the experimental section for DLS. Please see the supplementary information for the statistical analyses used in this study.

Differential centrifugal sedimentation

DCS measurements were performed using a disc centrifuge (model 24000UHR) from CPS Instruments Inc. 0.001 wt% solutions of PS220, PS330, PS410 particles were prepared in SEB and sonicated for ~30 minutes prior to measurement. The disc was loaded with a sucrose gradient comprising 2 – 8 wt% sucrose (Sigma Aldrich, 99 % pure) in SEB. The average density, refractive

index and viscosity values of the sucrose gradient fluid were assumed to be 1.02 g ml^{-1}, 1.361 and 1.2 cP, respectively. 0.5 ml of dodecane was added as an evaporation barrier and a disc rotational frequency of 24 000 rpm was used. The instrument was allowed to come to thermal equilibrium (~39 °C) before performing measurements. 100 µl of sample was injected into the disc for analysis. Measurements were performed in triplicate and a calibration measurement was performed before each run with a 355 nm polystyrene latex sample suspended in SEB. Particles were assumed to be spherical and have a refractive index of 1.59 and zero absorption. The calibration sample, PS220 and PS330 had a density of 1.06 g cm^{-3} while PS410 had a slightly lower density of 1.05 g cm^{-3} according to the manufacturers specifications. The proprietary CPS Instruments software (version 9.5) was used to generate the number-based PSD at <1 nm increments. Calculations of the mean, mode, CV% and percentile values were made from the frequency distribution data, with the frequency % values for the continuous absorbance values being used as weights, with a weighted degree of freedom, for the mean and CV% calculations. Please see the supplementary information for the statistical analyses used in this study.

Peak detection and data presentation

All statistical analysis and mathematical manipulation of the data was performed with Origin 8.0 or 8.6 software unless otherwise stated. The histograms and cumulative frequency plots presented in Figure 1, Figure 2 and Figure 3 are the averaged bin values of the replicates. Due to the way in which these 5 dissimilar techniques output the number-based PSD, it was not possible to visually present the PSDs of each technique with the same data formatting. The TEM, TRPSTRPS and PTA data are presented as histograms with 5 nm bins. The DLS data are presented as a number-based PSD histogram in logarithmically spaced size bins as defined by the proprietary GPM algorithm provided by Malvern Instruments. The DCS data are presented as a continuous measurement of detected particles with no data binning. Peak detection (Table 1) was performed using the Origin 8.0 peak detection algorithm for every replicate with data formatted as described above. Peak detection thresholds were set so that a peak would be detected if it had a height and width both greater than 5 % of the total data present after a manually fit baseline was applied.

Results and Discussion

Multimodal analysis: Technique resolution

To assess instrumental resolution and ability to discriminate between particulate samples that are of 1) high polydispersity, or 2) complex, multimodal distributions, we examined both monodisperse monomodal particle suspensions as well as a model ‘polydisperse’ multimodal suspension composed

of an equal weight mixture (1:1:1) of the monodisperse monomodal particle sets, PS220, PS330 and PS410. This multimodal suspension was considered suitable for testing system sensitivity for highly polydisperse samples as the monomodal populations are well defined according to TEM measurements, with arithmetic mean and CV% values of 209.7 nm ± 3.5 %, 321.8 nm ± 2.9 %, 411.7 nm ± 3.4 % for the PS220, PS330 and PS410 sets, respectively (see Table 2). These monodisperse particle sets provide little to no overlap of the three particle sets when measured as a mixed suspension, and a technique with high size resolution should be able to resolve the different populations. Additionally, the two fold increase in particle diameter across the multimodal suspensions allows for a good comparison of how well each technique handles samples with a broad range of particle sizes.

Figure 1 presents the averaged number-based PSDs of the replicate multimodal measurements made by DLS, TRPS, PTA and DCS. The single particle counting techniques, TRPS and PTA, are presented in 5 nm bins, whereas the ensemble technique, DLS, is presented as series of logarithmically spaced size bin values as is defined by the proprietary GPM algorithm provided by Malvern, and the separation technique, DCS, is presented as a continuous density distribution due to particles being detected in time as they pass across a light detector. To assess the ability of each technique to resolve the sub-populations present in the multimodal sample, a peak detection algorithm was used to detect the different populations of particles present and to provide PSD shape descriptors of the peak start, maximum, end, centroid and full width at half maximum (FWHM). The peak detection algorithm was used instead of manually identifying different particle populations and obtaining arithmetically derived PSD descriptors, such as percentile, mean and mode values, in order to remove human bias from the analysis, particularly in the event that the PSD of the three particle sets were to overlap in any of the measurements. The PSD shape descriptors obtained for each detected particle population were also compared to the corresponding values obtained from the monomodal measurements made by TEM and by each respective technique, which were also analyzed by the peak detection algorithm. These values are presented in Table 1 where multimodal and monomodal measurements are denoted by the "Multi" and "Mono" prefixes, respectively.

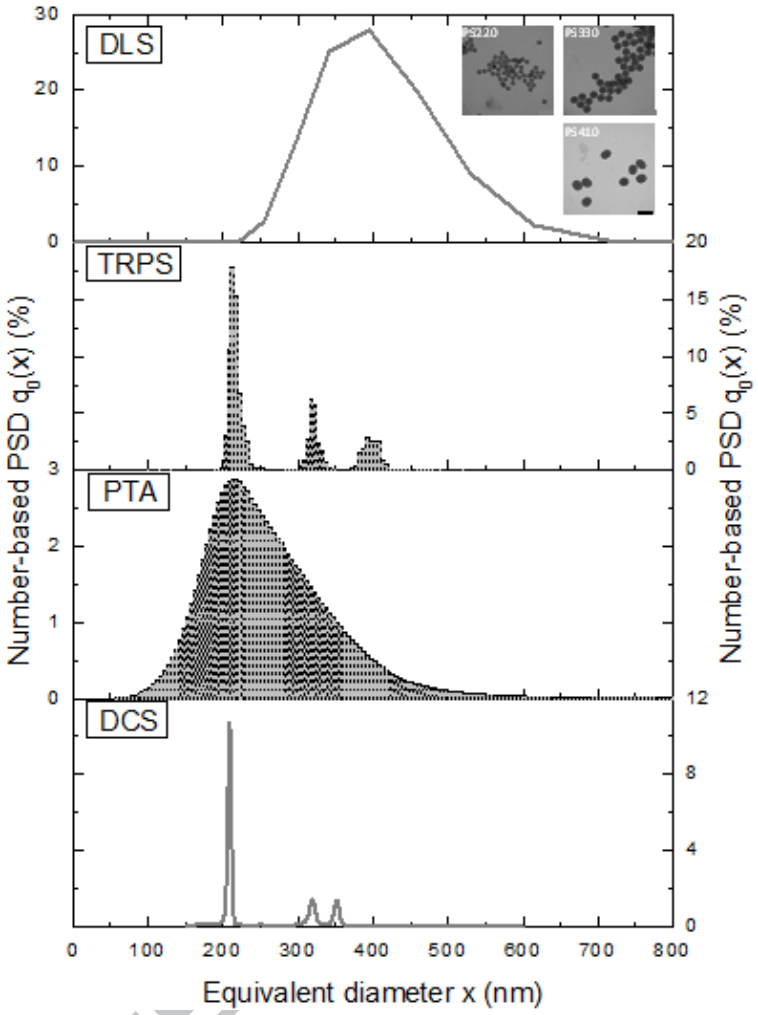

Figure 1. Averaged number-based PSDs obtained from triplicate analysis of the mixed 'multimodal' sample composed of PS220, PS330 and PS410 particles. The inset figure shows TEM images of the three separate particle sets. The scale bar represents 500 nm. The analysis resolution of the ENP and DCS techniques is sufficient to resolve the three particle sets within the mixture. DLS and PTA each give rise to a single broad peak that is skewed to the larger or smaller sized particles, respectively.

Table 1. Peak detection of the sub-populations in the multimodal distribution of PS220, PS330 and PS410 particles analyzed by DLS, TRPS and DCS. Values are the averages of the replicate measurements made, and values in brackets indicate standard deviations over the replicates made

Instrument	Population	Peak start (nm)	Peak max (nm)	Peak end (nm)	FWHM (nm)	Centroid (nm)	Peak integral
TEM	Mono PS220	182.5	207.5	232.5	13.1	209.4	
	Mono PS330	287.5	322.5	352.5	14.5	322.2	
	Mono PS410	357.5	417.5	447.5	16.8	411.7	
DLS	**Multi***	**227.2 (15.6)**	**396.1 (0)**	**712.4 (0)**	**195.1 (5.1)**	**412.7 (6.4)**	**100**
	Mono PS220	102.8 (19.4)	190.1 (0)	458.7 (0)	107.9 (3.9)	209.8 (0.9)	

	Mono PS330	164.2 (0)	295.3 (0)	531.2 (0)	186.1 (6.4)	337.1 (4.4)	
	Mono PS410	208.2 (16.5)	374.5 (29.6)	515.1 (0)	224.4 (6.9)	407.8 (2.1)	
TRPS	**Multi PS220**	**187.5 (5.0)**	**214.2 (2.9)**	**265.8 (11.5)**	**13.8 (0.3)**	**215.9 (0.7)**	**62.1**
	Mono PS220	199.2 (2.9)	219.2 (2.9)	289.2 (7.6)	20.6 (7.0)	225 (1.6)	
	Multi PS330	**290.8 (5.8)**	**320.8 (2.9)**	**352.5 (0)**	**12.7 (1.0)**	**320.8 (1.9)**	**21.4**
	Mono PS330	284.2 (10.4)	315.8 (2.9)	354.2 (7.6)	23.1 (1.9)	320.1 (3.6)	
	Multi PS410	**362.5 (5.0)**	**399.2 (7.6)**	**429.2 (7.6)**	**28.0 (2.0)**	**397.1 (2.0)**	**16.4**
	Mono PS410	360.8 (7.6)	402.5 (0)	454.2 (12.6)	29.9 (2.3)	398.9 (1.7)	
PTA	**Multi***	**70.8 (10.4)**	**212.5 (5.0)**	**502.5 (5.0)**	**156.2 (8.2)**	**256.8 (5.8)**	**100.0**
	Mono PS220	79.2 (2.9)	209.2 (2.9)	472.5 (5.0)	81.5 (1.2)	218.6 (0.4)	
	Mono PS330	130.8 (7.6)	305.8 (2.9)	497.5 (26.0)	93.8 (1.5)	306.9 (0.6)	
	Mono PS410	172.5 (0)	374.2 (2.9)	664.2 (2.9)	142.8 (2.4)	380.4 (1.8)	
DCS	**Multi PS220**	**168.3 (0.9)**	**209.6 (0.2)**	**225.4 (0.5)**	**5.3 (0)**	**208.6 (0.3)**	**69.2**
	Mono PS220	184.2 (11.5)	207.7 (0.1)	219.7 (2.1)	4.8 (0)	207.2 (0.3)	
	Multi PS330	**298.3 (0.6)**	**319.7 (0.5)**	**335.6 (0.1)**	**9.6 (0.4)**	**318.9 (0.1)**	**17.1**
	Mono PS330	265.1 (29.7)	317.6 (0.2)	333.5 (2.3)	8.3 (0.3)	315.5 (1.0)	
	Multi PS410[#]	**335.6 (0.1)**	**352.3 (0.8)**	**363.3 (1.0)**	**8.6 (0.1)**	**351.7 (0.8)**	**13.7**
	Mono PS410[^]	359.6 (26.1)	402.9 (1.2)	426.5 (4.6)	8.6 (0.5)	402.0 (1.3)	

Expected Integrals for the PS220, PS330 and PS410 sub populations were 69.6 %, 19.6 % and 10.8 %, respectively

*Only 1 peak detected for the multimodal suspensions with this technique

#These measurements were made assuming a density of 1.06 g/cm^3 for the PS410 multimodal sample. Rerunning the measurements and using the correct density of 1.05 g/cm^3, these values were 387.5 (0.2), 406.8 (1.0), 419.8 (1.2), 9.9 (1.4), 406.1 (1.0) from left to right.

^A density of 1.05 g/cm^3 was used to calculate these values.

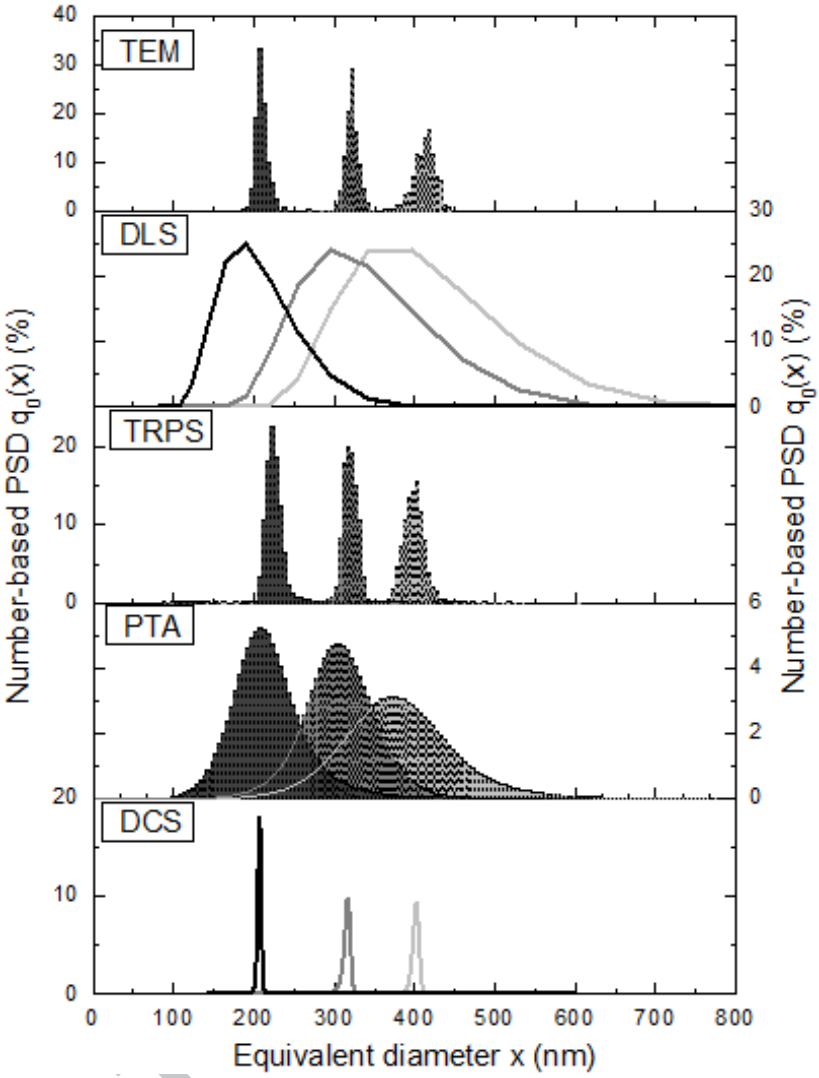

Figure 2. Averaged number-based PSDs obtained from the unmixed 'monomodal' analysis of PS220, PS330 and PS410 particle samples. DLS and DCS graphs are presented as lines as they are an ensemble and continuous technique, respectively. All techniques generated very similar mean size values, however large discrepancies in the PSD width were observed with the light scattering techniques (DLS and PTA) which gave to the broadest PSDs.

Of the four techniques, only TRPS and DCS had sufficient resolution to detect the three particle sets present in the mixed multimodal suspension, with each clearly present in the number-based PSDs (Figure 1). Except for the peak corresponding to the PS410 particles in the DCS measurement, all the other peak maximum (mode) values reported by TRPS and DCS were within 5 % of the TEM measured reference values and 2.5 % of their equivalently unmixed monomodal values. The slightly smaller than expected (~65 nm smaller) value in the DCS measurement was the result of a difference in the density of the PS220, PS330 (1.06 g/cm^3) and the PS410 (1.05 g/cm^3) particle sets (densities

obtained from the manufacturer). The lower density of the PS410 resulted in under sizing by DCS, as density affects particle sedimentation according to Stokes law (Equation 4). This highlights a critical disadvantage to the DCS technique in that the PSD is highly dependent on the ascribed particle density. Samples which contain particles of different densities, or where the particle density is unknown, or there is a very small error in the assumed density, will result in significant errors in the measured PSD. Recalculating the data with a 1.05 g/cm^3 density value for the particle sets produced the exact opposite trend (not shown), shifting the PS410 peak towards the expected size, but in turn also increased the measured sizes of the PS220 and PS330 sets by ~50-60 nm.

Both light scattering/Brownian motion based techniques, DLS and PTA, failed to detect more than a single peak in their analysis of the multimodal suspension, indicating that these techniques do not have the resolution required to detect the PSD of this complex multimodal sample. The detected peak maximum value for the DLS measurement was within 5.2 % and 5 % of the PS410 TEM and monomodal DLS measurement peak maximum values, respectively. Additionally, the peak start, end, FWHM and centroid values of the single peak detected in the multimodal measurement were within 15% of the monomodal DLS measurement of the PS410 particle set, further indicating that only the larger PS410 nm set was detected by DLS. This trend was expected, and has been reported previously in the literature, as light scattering techniques are known to be biased towards detecting larger particles within polydisperse suspensions [25, 27]. All DLS data in the main text of this manuscript has been analyzed using Malvern's GPM algorithm. For a discussion of the data by the higher resolution MNM algorithm please see the supplementary information section "MNM analysis of multimodal DLS measurements". PTA was also found to lack the resolution to distinguish between the three particle populations within the mixed multimodal sample. Closer visual inspection of the multimodal histogram appears to indicate that PTA was able to detect the other two particle sets (PS330 and PS410) present in the sample. Despite the peak maximum remaining the same as the PS220 measurement (within ~1.6 %), broadening of the PSD towards the larger particles present in the multimodal sample can be seen in the peak start, peak end, FWHM and centroid values, which all indicated a broadening of the PSD when compared to the PS220 monomodal measurement. In contrast to the DLS data, the broad PSD histogram generated by PTA was instead skewed to preferentially detecting the smaller particle set. This is due to the higher concentration of smaller particles in the sample, which is a result of the mixing of particle sets by a 1:1:1 weight ratio. Measuring the same particle sets in a weight ratio of 1:2:2 for the PS220, PS330 and PS410 particle sets produced a distribution (see supplementary information Figure S2) that was shifted towards the larger particles in the sample, with a peak maximum of 294 nm. This indicates that while PTA is a lower resolution technique than DCS or TRPS, all particles present in the multimodal sample will

affect the measurement, unlike DLS. A discussion on how the proprietary Nanosight algorithm may affect the resolution accuracy and precision of a PSD measurement is beyond the scope of this paper, however a more detailed discussion on the PTA algorithm is available in reference [6].

Figure 3**Error! Reference source not found.** overlays the TEM P10-P90 percentile range (grey bars) of each particle set on top of the cumulative number-based PSDs measured by each technique for the multimodal sample. It is clear that the TRPS measurement was best able to detect the three particle populations. DCS was also highly accurate, however as described earlier, the PS410 particles were undersized due to their lower density. As was obvious in the histogram presented in Figure 1, DLS and PTA do not offer the resolution to distinguish the three separate particle sets.

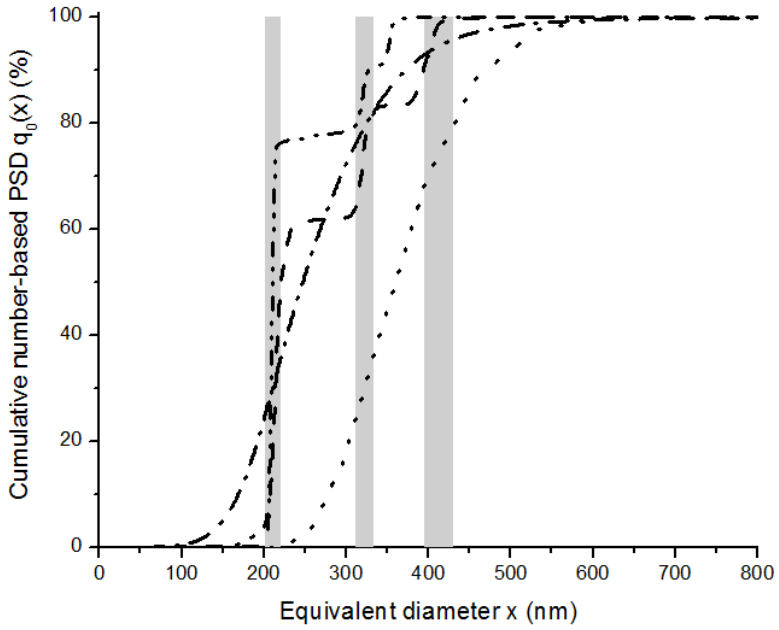

Figure 3. Averaged cumulative number-based PSDs of the multimodal PS220, PS330 and PS410 particles. DLS (dot), TRPS (dash), PTA (dash-dot), DCS (dash-dot-dot). The shaded areas indicate the P10, P50 and P90 values from the TEM measurements of the PS220, PS330 and PS410 particle sets and are provided for comparison of the five techniques.

In addition to resolving the individual particle sets, the number fraction of each of the measured peaks, obtained by integrating the PSD for each peak, correlated very well to the expected relative amount of particles within the 1:1:1 wt% stock solutions. From the particle size and density the 1:1:1 wt% solution is expected to contain PS220, PS330 and PS410 particles in a total number percent ratio of 69.5:19.5:11%, respectively. TRPS and DCS analysis of the averaged multimodal replicates produced population percentages of 62.1%, 21.4% and 16.4% and 69.2%, 17.1% and 13.7% for PS220, PS330 and PS410, respectively. This indicates that for these two techniques there

was no skewing of the data based on the particle size or concentration. However, due to the large number of errors that may exist in these calculations and experiments, i.e., the random errors associated with the stock concentration, errors in dilutions and the broadness of the PSD, it is hard to form any clear conclusions from this brief analysis on size/concentration dependent particle selectivity for these techniques. It should be noted that the method used above to obtain relative information about the ratio of the different concentrations in a sample is similar to the method used by TRPS to obtain qualitative concentration measurements [46], using a concentration standard to measure an unknown sample.

It is worth noting that that the single particle nature of the TRPS and PTA techniques can result in a small subpopulation in a sample being missed when an insufficient number of particles are analyzed. In this study, a minimum of 2000 individual particles were measured for each of the TRPS replicate measurements in the multimodal sample to obtain a good representation of each population. Direct observation of the particles in the PTA measurement ensured all three particle populations were present. However, if a small outlier population of particles were to be present in a sample where no *a priori* knowledge of the PSD is available, then it is possible that the small number of particles being measured will not produce a PSD that is representative of the sample. For normal or log normal monomodal samples, statistical analysis of the PSD data from a single particle measurement technique can be made to ascertain the level of confidence in the obtained PSD shape [47], however, in the case of a multimodal system this becomes non-trivial. Additionally, this form of analysis requires an assumption of normality for the PSD, and as discussed in the supplementary information (see "Assessment of normality of TEM data" for more information), this is potentially not the case for the particle sets used in this study.

Measurement accuracy and precision

The accuracy of the two techniques that were able to detect the three particle populations in the multimodal suspension, TRPS and DCS, was assessed by comparing the averaged replicated peak detection values (peak start, maximum and end, centroid and FWHM), from both the multimodal and monomodal measurements, to the corresponding values obtained from reference TEM measurements. The deviation of these PSD descriptors between multimodal and monomodal measurements was also assessed. For the techniques that were not able to detect the three particle populations in the multimodal sample, DLS and PTA, accuracy was assessed by comparing the PSD percentile values at 10, 50 and 90 % (P10, P50, P90), the arithmetic mean and the CV% values from the monomodal measurements to the TEM measurement (This analysis was also performed for the monomodal TRPS and DCS measurements). These results are presented in Table 2. To simplify this assessment, only deviations that are consistent across several measurements by a technique (being greater than 5 % for the comparison at hand) were considered to be significant and are discussed. Precision was assessed from the standard deviation of these values over the replicate measurements made for both the multimodal and monomodal data.

Table 2. Shape descriptors for PSDs obtained from monomodal analysis. Values are the averages of the 3 or 5 replicate measurements made (depending on the technique), and values in brackets indicate standard deviations over the replicates made.

Sample	System	Mean (nm)	CV (%)	P10	P50	P90
PS220	TEM	209.7	3.5	201.5	208.7	219.5
	DLS	197.3 (1.3)	23.8 (1.3)	141.8 (0.0)	190.1 (0.0)	255.0 (0.0)
	TRPS	225.3 (2.1)	7.2 (1.7)	213.8 (3.7)	223.5 (1.5)	237.2 (1.0)
	PTA	219.9 (0.6)	23.2 (0.5)	165.7 (0.6)	214.0 (1.0)	277.7 (1.5)
	DCS	207.4 (1.4)	5.3 (2.6)	203.9 (0.6)	207.4 (0.2)	210.3 (0.3)
PS330	TEM	321.8	2.9	312.1	321.9	333.0
	DLS	323.7 (4.6)	23.9 (1.4)	241.1 (19.4)	295.3 (0.0)	446.2 (28.0)
	TRPS	319.3 (3.7)	6.5 (1.2)	309.8 (3.1)	319.6 (3.8)	331.8 (3.9)
	PTA	307.4 (0.6)	15.0 (0.4)	251.3 (2.1)	307.0 (1.0)	364.3 (0.6)
	DCS	313.1 (1.1)	6.8 (2.2)	306.5 (0.7)	316.6 (0.1)	321.5 (0.1)
PS410	TEM	411.7	3.4	394.6	413.4	428.8
	DLS	396.1 (2.2)	23.2 (1.2)	295.3 (0.0)	396.1 (0.0)	531.2 (0.0)
	TRPS	392.9 (1.4)	10.7 (1.4)	380.2 (2.2)	398.4 (0.9)	415.4 (5.3)
	PTA	381.7 (1.8)	18.8 (0.3)	296.7 (1.2)	377.7 (1.5)	469.7 (2.5)
	DCS	399.6 (3.7)	6.9 (3.7)	393.9 (2.4)	402.3 (1.1)	407.5 (0.8)

Peak maximum and centroid values in the TRPS and DCS measurement where found to agree well between both the multimodal, monomodal and reference TEM measurements, with most values

falling within 5% of each other. However consistent deviations between measurements were seen in PSD width description values such as the peak start and FWHM. Of note were the TRPS monomodal FWHM values, which deviated greatly from the TEM values, with the PS220, PS330 and PS410 values deviating by 56.8, 58.7 and 9.5 %, respectively. These deviations may be due to the single particle measurement nature of the TRPS technique, as discussed in the "multimodal analysis" section, where the PSD may vary significantly in both these techniques due to the small number of particles that are measured. The FWHM values in both the monomodal and multimodal DCS measurements also deviated significantly, being significantly smaller, and therefore indicating a much thinner PSD, than the TEM measurements by 63.6, 43.0 and 68.6 % in the monomondal measurement and by 59.5, 34.0 and 63.6 % in the multimodal measurements for the PS220, PS330 and PS410 measurements, respectively. It is possible that the DCS settings were not optimal for this sample, preventing higher resolution size separation of the individual particle sets. Alternatively, having been obtained on in situ samples, where the a number of particles "measured" is many orders of magnitude larger than what has been measured by TEM, where material inhomogeneity in the particles and factors such as disruption of the particles by the electron beam and *in vacuo* conditions may result in a broadening of the observed PSD, it could be argued that the DCS measurement is instead offering a truer representation of the PSD. These aspects could be investigated by varying the speed of the disc, or altering the density gradient, so that the retention time of a well characterized sample can be altered to study its effects on the measured PSD.

Interestingly, significant deviations were also observed in some peak start and FWHM values when comparing intra-instrument measurements of the multimodal and monomodal samples performed by TRPS and DCS. The multimodal FWHM measurements made by TRPS deviated significantly from the single modal measurements by 32.7, 45.2 and 6.4 % for the PS220, PS330 and PS410 particle sets, respectively. Again, this deviation in FWHM values in the TRPS measurements can best be explained by the relatively small number of particles measures in this single particle technique. The monomodal DCS PS220, PS330 and PS410 (when adjusted for a density of 1.05 g/cm^3) FWHM values were all significantly smaller than the multimodal data by 11.2, 15.8 and 15.9 %, respectively and consistent deviations in the detected peak start values between the multimodal and monomodal measurements were seen for all three particle populations, (PS220 (8.6 %), PS330 (12.5 %) PS410 (7.8 %)). We can currently find no obvious reason why these deviations in the DCS measurements occurred other than inter-measurement variation.

Due to the lack of resolution of the DLS and PTA techniques, where only one particle population in the multimodal sample was detected, directly comparing the accuracy of these techniques to the

monomodal and reference TEM measurements was not possible by means of the peak detection algorithm. However, it was possible to obtain a measure of the accuracy of these techniques by comparing the P10, P50, P90, arithmetic mean and CV% values obtained from the monomodal measurements of each particle set to the reference TEM values. The accuracy of the TRPS and DCS techniques was also assessed in this manner. The P50 (modal) and arithmetic mean values for all techniques were shown to be fairly accurate, being within 10 % of the reference TEM values. In contrast, the shape of the PSDs measured varied greatly over the different techniques, as can be seen in the wide range of P10, P90 and CV% values, and visually in the monomodal measurement graphs presented in Figure 2. DLS and PTA had the greatest deviation in the P10 and P90 measurements, ranging from ~8 % to ~30 % deviation from the TEM measurements. The wider PSDs measured by DLS and PTA resulted in CV% values of the PS220, PS330 and PS410 particles that were far greater than the TEM measurements, being ~580 %, ~730 %, ~580 % greater for the DLS and ~561 %, ~420 %, ~450 % for PTA. These large CV% values highlight the low resolution of these two techniques. In contrast, the TRPS and DCS measurements were much closer to the TEM measurements, with deviations in the P10 and P90 values typically being less than 5 %. The CV% values for the TRPS and DCS measurements were also much smaller than the DLS and PTA values, however, they were still significantly larger than the TEM values, deviating by ~105 %, ~125 %, ~214 % for the TRPS and ~50 %, ~130 %,~100 % for the DCS measurements for the PS220, PS330 and PS410 samples, respectively. For further discussion as to why these higher resolution techniques observed broader than expected PSDs, please see supplementary information "CV% broadness in monomodal TRPS and DCS measurements".

All of the techniques were found to have high measurement precision as defined by the standard deviation of the PSD shape values over the replicate measurements of both the monomodal and multimodal measurements. This measurement precision is demonstrated by the small standard deviations in the peak detection measurements of both the monomodal and multimodal data (Table 1) and in P10, P50, P90, CV% and arithmetic mean values for the monomodal data (Table 2). The standard deviations of the P10, P50 and P90 are also presented graphically as error bars in the cumulative frequency plots in Supplementary Information Figure S3. Most PSD shape descriptor values had standard deviations below 5 nm. Several particularly large deviations were seen in the the monomodal DLS measurement of the PS330 particle set, where the P10 and P90 values had standard deviations of 19.4 nm and 28.0 nm, respectively. These deviations were the result of the low resolution, logarithmically-spaced bins produced by the GPM algorithm, where the P10 and P90 values fell on either side of a bin division over the replicates made. Similar results can be seen in the peak detection values in Table 1.

There are also several instances where the PSD shape values in the DLS data were the same over all replicates due to the low resolution bins, resulting in a standard deviation of zero. Standard deviations of zero in the PSD shape values in other techniques were less likely to occur due to the smaller bin sizes or single particle nature of the techniques, allowing for higher resolution in the measurement, but greater deviation in the calculation of the percentile values. In the TRPS and PTA data there were some larger deviations of ~10 nm seen in the peak start and end values in both the monomodal and multimodal measurements. These deviations were most likely due to the low number of particles being measured in these techniques, resulting in greater deviation at the 5% peak threshold values used in the in the peak detection algorithm. However, despite only measuring several hundreds of particles, both the TRPS and PTA techniques typically gave highly reproducible PSD shape values when analyzed at the 5 nm bin level. The DCS measurements only showed larger than 5 nm deviations in the peak start values of the monomodal measurements and is most likely the result of baseline noise effecting the peak detection algorithm.

Conclusion

Of the four techniques compared in this study, the multimodal measurements made by TRPS and DCS were consistently found to surpass the measurements made by DLS and PTA. TRPS and DCS provided the greatest resolution and accuracy, being the only techniques to distinguish the peak maximum (modal) values of the 220, 330 and 410 nm sub-populations present within the multimodal sample to within 5% of the TEM reference measurements (after density corrections in the DCS measurement). However, variations in the PSD shape descriptors, such as the P10, P90 and FWHM values, were observed when comparing the TRPS and DCS measurements to the reference TEM measurements. It is possible that the limited number of particle measured in the TEM reference may be artificially overstating the error in these techniques due to the increased uncertainty in the PSD. If this is the case, then the large quantity of particles measured by DCS, or potentially, a TRPS measurement with a substantially larger particle count, may provide a more accurate measure of the true PSD present in the multimodal sample. Unfortunately, a study to ascertain these claims would be incredibly time consuming and is beyond the scope of this investigation.

The failure of DLS and PTA to identify the sub-populations present in the multimodal sample suggest that these two techniques offer a lower resolution of analysis. More importantly this inability to resolve the particle sets reduced the reported measurement accuracy. Thus, as the DLS measurements made no indication that the sample was multimodal in any way, it is a recommendation of this study that DLS only be used where *a priori* knowledge of the samples

monodispersity is known or, if this is not possible, that DLS be combined with single particle or separations based techniques, such as TRPS, TEM or DCS. Interestingly, despite being a single particle technique, PTA did not offer the resolution to distinguish between the three particle sets in the multimodal sample, however, there was evidence based on the broadness and skewing of the PSD, and from directly observe the particles being analyzed, that a highly polydisperse sample was under analysis. In such situations, a skilled user should be able to conclude whether further analysis of the sample by a higher resolution techniques is necessary.

In single modal measurements of the three particle sets, all of the techniques were able to easily identify the monomodal samples and gave similar average particle diameters when compared to the values obtained by TEM, however the broadness of the distributions varied greatly between three techniques, particularly for DLS and PTA, where the PSDs were far broader than the TEM reference measurements. Combined with the inability to distinguish the three particle populations present in the multimodal samples, these broad distributions further reinforced the lower resolution of these two light detection techniques. The precision of each technique was good, with little variation in the PSDs observed for replicate measurements.

Despite the promising results from DCS and TRPS, the substantial variation in the PSDs obtained from these four, fundamentally different, commercial techniques, suggests that the process of obtaining an accurate PSD of a highly polydisperse sample is still a complicated and time consuming process. As this study only offers a preliminary assessment of the capabilities of the assessed techniques, without further investigations to thoroughly assess the benefits and limitations of each technique it is a conclusion of this study that the PSD of complex samples must be investigated thoroughly, by several techniques before comments on the PSD can be made.

Acknowledgements

The authors acknowledge the scientific equipment provided by Izon Science Ltd.

The authors acknowledge the facilities, and the scientific and technical assistance, of the Australian Microscopy & Microanalysis Research Facility at the Centre for Microscopy and Microanalysis, The University of Queensland.

References

[1] M. Gaumet, A. Vargas, R. Gurny, F. Delie, Eur. J. Pharm. Biopharm. 69 (2008) 1-9.

[2] A. Braun, O. Couteau, K. Franks, V. Kestens, G. Roebben, A. Lamberty, T.P.J. Linsinger, Adv. Powder Technol. 22 (2011) 766-770.

[3] R.C. Woodward, J. Heeris, T.G. St. Pierre, M. Saunders, E.P. Gilbert, M. Rutnakornpituk, Q. Zhang, J.S. Riffle, J. Appl. Crystallogr. 40 (2007) s495-s500.

[4] O. Elizalde, G.P. Leal, J.R. Leiza, Part. Part. Syst. Charact. 17 (2000) 236-243.

[5] L.A. Fielding, O.O. Mykhaylyk, S.P. Armes, P.W. Fowler, V. Mittal, S. Fitzpatrick, Langmuir 28 (2012) 2536-2544.

[6] N.C. Bell, C. Minelli, J. Tompkins, M.M. Stevens, A.G. Shard, Langmuir 28 (2012) 10860-10872.

[7] D.G. Rickerby, G. Valdrè, U. Valdrè, Impact of electron and scanning probe microscopy on materials research. Kluwer Academic Publishers, Dordrecht ; Boston, 1999.

[8] International Organization for Standardization, ISO 13322-1:2004 Particle size analysis -- Image analysis methods -- Part 1: Static image analysis methods, 2004

[9] W. Rasband, ImageJ (computer program), National Institute of Health,

[10] M. Cybernetics, Image-Pro Plus (computer program), Roper Industries,

[11] L. Marton, Nature 133 (1934) 911-911.

[12] R. Finsy, Adv. Colloid Interface Sci. 52 (1994) 79-143.

[13] W. Brown, Dynamic light scattering: the method and some applications. Clarendon Press, the University of Michigan, 1993.

[14] Å.K. Jamting, J. Cullen, V.A. Coleman, M. Lawn, J. Herrmann, J. Miles, M.J. Ford, Adv. Powder Technol. 22 (2011) 290-293.

[15] C.M. Hoo, N. Starostin, P. West, M.L. Mecartney, J. Nanopart. Res. 10 (2008) 89-96.

[16] W.H. Coulter, Means for Counting Particles Suspended in a Fluid, U.S. Patent 2656508

[17] D. Kozak, W. Anderson, R. Vogel, M. Trau, Nano Today 6 (2011) 531-545.

[18] R.R. Henriquez, T. Ito, L. Sun, R.M. Crooks, Analyst 129 (2004) 478-482.

[19] C. Dekker, Nat. Nanotechnol. 2 (2007) 209-215.

[20] H. Bayley, C.R. Martin, Chem. Rev. 100 (2000) 2575-2594.

[21] R.W. Deblois, C.P. Bean, Rev. Sci. Instrum. 41 (1970) 909-914.

[22] S.J. Sowerby, M.F. Broom, G.B. Petersen, Sens. Actuators, B 123 (2007) 325-330.

[23] D. Upadhyay, S. Scalia, R. Vogel, N. Wheate, R. Salama, P. Young, D. Traini, W. Chrzanowski, Pharm Res 29 (2012) 2456-2467.

[24] G.S. Roberts, D. Kozak, W. Anderson, M.F. Broom, R. Vogel, M. Trau, Small 6 (2010) 2653-2658.

[25] D. Kozak, W. Anderson, M. Grevett, M. Trau, J. Phys. Chem. C 116 (2012) 8554-8561.

[26] R. Vogel, G. Willmott, D. Kozak, G.S. Roberts, W. Anderson, L. Groenewegen, B. Glossop, A. Barnett, A. Turner, M. Trau, Anal. Chem. 83 (2011) 3499-3506.

[27] G.R. Willmott, M.F. Broom, M.L. Jansen, R.M. Young, W.M. Arnold, in: O. Hayden, K. Nielsch(Eds), Springer US, 2011, p 209-261.

[28] V. Filipe, A. Hawe, W. Jiskoot, Pharm. Res. 27 (2010) 796-810.

[29] K. Braeckmans, K. Buyens, W. Bouquet, C. Vervaet, P. Joye, F. De Vos, L. Plawinski, L. Doeuvre, E. Angles-Cano, N.N. Sanders, J. Demeester, S.C. De Smedt, Nano Lett. 10 (2010) 4435-4442.

[30] H. Lamb, Hydrodynamics. 6th ed., Dover publications, New York, 1945.

[31] CPS Disc Centrifuge Operating Manual, CPS Instruments, Inc., Florida, 2006

[32] I. Laidlaw, M. Steinmetz, in: D.J. Scott, S.E. Harding, A.J. Rowe(Eds), Analytical Ultracentrifugation - Techniques and Methods, Royal Society of Chemistry, 2005, p 270-290.

[33] H. Ruf, B.J. Gould, W. Haase, Langmuir 16 (2000) 471-480.

[34] G.S. Roberts, S. Yu, Q. Zeng, L.C. Chan, W. Anderson, A.H. Colby, M.W. Grinstaff, S. Reid, R. Vogel, Biosens. Bioelectron. 31 (2012) 17-25.

[35] K. Sommer, Sampling of powders and bulk materials. Springer-Verlag, Berlin ; New York, 1986.

[36] N.G. Stanley-Wood, R.W. Lines, Particle Size Analysis. The Royal Society of Chemistry, Cambridge, 1992.

Highlights

- The accuracy of particle size distribution measurements is technique dependent.
- The disparity between measurements made by different techniques increases with sample complexity and polydispersity.
- Only TRPS and DCS techniques resolved all particles present in complex multimodal samples.
- PTA and DLS techniques had lower resolution and reported higher polydispersity than truly present in all test samples.
- All four techniques tested had high repeat measurement precision.